

## The temperature of an optically trapped, rotating microparticle

Paloma Rodríguez Sevilla, Yoshihiko Arita, Xiaogang Liu, Daniel Jaque, and Kishan Dholakia

*ACS Photonics*, **Just Accepted Manuscript** • DOI: 10.1021/acsp Photonics.8b00822 • Publication Date (Web): 09 Aug 2018

Downloaded from <http://pubs.acs.org> on August 10, 2018

### Just Accepted

“Just Accepted” manuscripts have been peer-reviewed and accepted for publication. They are posted online prior to technical editing, formatting for publication and author proofing. The American Chemical Society provides “Just Accepted” as a service to the research community to expedite the dissemination of scientific material as soon as possible after acceptance. “Just Accepted” manuscripts appear in full in PDF format accompanied by an HTML abstract. “Just Accepted” manuscripts have been fully peer reviewed, but should not be considered the official version of record. They are citable by the Digital Object Identifier (DOI®). “Just Accepted” is an optional service offered to authors. Therefore, the “Just Accepted” Web site may not include all articles that will be published in the journal. After a manuscript is technically edited and formatted, it will be removed from the “Just Accepted” Web site and published as an ASAP article. Note that technical editing may introduce minor changes to the manuscript text and/or graphics which could affect content, and all legal disclaimers and ethical guidelines that apply to the journal pertain. ACS cannot be held responsible for errors or consequences arising from the use of information contained in these “Just Accepted” manuscripts.

# The temperature of an optically trapped, rotating microparticle

Paloma Rodríguez-Sevilla,<sup>\*,†</sup> Yoshihiko Arita,<sup>†,‡</sup> Xiaogang Liu,<sup>¶</sup> Daniel Jaque,<sup>§</sup>  
and Kishan Dholakia<sup>\*,†,||</sup>

<sup>†</sup>*SUPA, School of Physics and Astronomy, University of St Andrews, North Haugh, Fife,  
KY16 9SS, United Kingdom.*

<sup>‡</sup>*Molecular Chirality Research Center, Chiba University, 1-33 Yayoi-cho, Inage-ku,  
Chiba-shi 263-0022, Japan.*

<sup>¶</sup>*Department of Chemistry National University of Singapore Science Drive 3, Singapore  
117543, Singapore.*

<sup>§</sup>*Fluorescence Imaging Group Departamento de Física de Materiales Universidad  
Autónoma de Madrid 28049 Madrid, Spain and Nanobiology Group Instituto Ramón y  
Cajal de Investigación Sanitaria Hospital Ramón y Cajal. Ctra. De Colmenar Viejo Km.  
9100, 28034 Madrid, Spain.*

<sup>||</sup>*Graduate School of Science and Engineering, Chiba University, 1-33 Yayoi-cho, Inage-ku,  
Chiba-shi 263-0022, Japan.*

E-mail: prs8@st-andrews.ac.uk; kd1@st-andrews.ac.uk

Phone: +44 (0)1334 463184

## Abstract

The measurement of temperature at the mesoscopic scale is challenging but important in a wide variety of research fields, including the investigation of single molecule and cell mechanics and interactions as well as fundamental studies in heat transfer and Brownian

1  
2  
3 dynamics on this scale. In this letter we present a route that determines temperature  
4 at the nano- to microscale with three independent measurements performed on a single  
5 trapped, rotating luminescent microparticle. We measure temperature changes using  
6 both the internal and external degrees of freedom, via (i) the upconverted luminescence,  
7 (ii) the rotation rate, and (iii) the Brownian dynamics of the particle. This novel  
8 tripartite approach allows us to cross-correlate the temperature for both the internal and  
9 external (center-of-mass) degree of freedom for the particle. In addition, our approach  
10 provides a measure of the temperature increase without the need of a precise knowledge  
11 of the particle dimensions, shape or any previous calibration of the sample or the  
12 experimental set-up. The developed technique opens up prospects for stringent tests of  
13 nanothermometry.  
14  
15  
16  
17  
18  
19  
20  
21  
22  
23

## 24 25 26 **Keywords** 27

28  
29 optical trapping; upconverting particles; birefringence; optical torque; nanothermometry  
30  
31  
32

33 The measurement of temperature at high resolution plays an important role in numerous  
34 processes, particularly at mesoscopic spatial scales. Micro and nanoparticle dynamics within  
35 a fluid are subject to Brownian motion, and as such, the particle's external degrees of freedom  
36 (translation and rotation) are strongly influenced by temperature due to their dependence  
37 on the viscosity of the surrounding medium.  
38  
39  
40  
41  
42

43 Optical tweezers offer an ideal platform to study Brownian dynamics since the optical  
44 forces and torques acting on a trapped particle are counteracted and balanced by the forces  
45 and torques from the environment, which may also act as a method of heat dissipation. By  
46 recording the motion of a Brownian particle trapped in liquid, it is possible to probe the  
47 local fluid viscosity and its corresponding temperature around the particle. Recently much  
48 effort has been directed at cooling the center-of-mass (CoM) motion of trapped particles  
49 in vacuum, where the Brownian motion is controlled by optical fields,<sup>1-4</sup> with a view to  
50  
51  
52  
53  
54  
55  
56  
57  
58  
59  
60

1  
2  
3 reaching the quantum ground state. Within this context, the temperature of the particle is  
4 often assumed to be exclusively determined by its CoM motion (external degree of freedom)  
5 based on the equipartition theorem.  
6  
7

8  
9 On the other hand, upconverting particles (UCPs), have recently brought a surge of in-  
10 terest in a variety of fields ranging from biological studies to quantum physics. UCPs are  
11 able to absorb two or more incident photons of relatively low energy and convert them into  
12 one emitted photon with higher energy, through a process known as upconversion (UC).<sup>5-7</sup>  
13 Importantly, the emission spectrum of a UCP encodes information of its *internal tempera-*  
14 *ture*.<sup>8</sup> When a UCP is optically trapped with a continuous wave (cw) beam at an appropriate  
15 excitation wavelength it can be used as a remotely controlled thermometer.<sup>9,10</sup> Furthermore,  
16 depending on the doping type/content and the incident excitation wavelength, UCPs can  
17 be either refrigerated or heated,<sup>11,12</sup> thus offer an interesting testbed to measure and control  
18 both the internal and CoM temperature.  
19  
20  
21  
22  
23  
24  
25  
26  
27  
28

29 Previous studies have shown that the internal temperature of a particle is in fact coupled  
30 to the CoM temperature.<sup>4,13</sup> Recently, laser-induced refrigeration of an optically trapped  
31 Yb-doped UCPs has been reported both in liquid<sup>14</sup> and vacuum.<sup>11</sup> These studies show that  
32 the CoM temperature of the particle is comparable with its internal temperature within  
33 experimental errors. However, these studies do not offer any detailed analysis of how these  
34 internal and external temperatures compare in the context of micro- or nano-thermometry.  
35 Intriguingly, a recent study looked at coupling between internal and external degrees of  
36 freedom of a vacuum trapped nanoparticle.<sup>4</sup> Heating by the laser and black-body radiation  
37 were attributed to lead to an internal temperature ( $> 1000$  K) well in excess of the CoM  
38 temperature ( $< 10$  K), even in the presence of parametric feedback cooling. Such studies are  
39 the cornerstone for future levitated hybrid optomechanics experiments. Importantly high  
40 internal particle temperatures can adversely affect studies of such particles at the classical-  
41 quantum interface and lead to a reduction in their performance as an ultra-precise sensor.  
42  
43  
44  
45  
46  
47  
48  
49  
50  
51  
52  
53  
54

55 In this study we propose a novel tripartite method able to independently measure and  
56  
57  
58  
59  
60

1  
2  
3 correlate temperature changes from both the external and internal degrees of freedom for  
4 a single trapped UCP. Two different types of UCPs, one with high absorption and the  
5 other with lower absorption at the trapping wavelength, are employed. The dissipation of  
6 the absorbed energy occurs through non-radiative processes mediated by phonons in the  
7 material structure which produces a temperature increment only for the highly-absorbing  
8 particles. To demonstrate our approach we measure the temperature of a single UCP trapped  
9 in water. Firstly, the luminescent spectrum is recorded to determine the particle's internal  
10 temperature. This contrasts with other approaches <sup>4</sup> where a detailed knowledge of the  
11 particle material properties are required. This is then compared with the external (CoM)  
12 temperature of the UCP determined from the particle dynamics (translational and rotational  
13 degrees of freedom) directly linked to the viscosity changes of the environment.  
14  
15  
16  
17  
18  
19  
20  
21  
22  
23  
24

25 A key attribute to distinguish our presented tripartite approach is that it does not require  
26 any knowledge of the particle physical properties, such as shape and size, or any calibration  
27 of the sample or the experimental system. Furthermore, our experimental errors are much  
28 smaller than those previously reported in aqueous media,<sup>14-16</sup> allowing us to provide a strin-  
29 gent approach for the analysis of heat transfer at the microscale for such optically trapped  
30 particles.  
31  
32  
33  
34  
35  
36  
37  
38  
39

## 40 Experimental

41  
42 **Thermometers.** Two differently doped UCPs were used in this study:  $\text{NaYbF}_4:\text{Er}^{3+},\text{Nd}^{3+}$   
43 and  $\text{NaYF}_4:\text{Er}^{3+},\text{Yb}^{3+}$  microcrystals (see Methods for details). They present a similar disc-  
44 like shape with hexagonal facets, as shown in the scanning electron microscope (SEM) images  
45 of Figures 1(a) and 1(b). In addition, both samples exhibit light emission in the visible range  
46 under near-infrared 788 nm excitation. Figures 1(c) and 1(d) show the normalized lumines-  
47 cence spectrum associated to the green emission of Er ions obtained from a single optically  
48 trapped  $\text{NaYbF}_4:\text{Er}^{3+},\text{Nd}^{3+}$  and  $\text{NaYF}_4:\text{Er}^{3+},\text{Yb}^{3+}$  particle, respectively. Importantly, the  
49  
50  
51  
52  
53  
54  
55  
56  
57  
58  
59  
60

1  
2  
3 relative emission intensity of the bands centered around 520 nm and 540 nm is temperature  
4 dependent due to the change in the electronic population of the thermally-coupled excited  
5 states with temperature (see Supporting Information for details).<sup>8,17,18</sup> For our study, only  
6 the highlighted bands in Figures 1(c) and 1(d) were used in order to reduce the experimental  
7 error in the determination of the thermal changes (see Supporting Information for details).  
8 In order to show the capability of the developed tripartite method to measure temperature  
9 changes for a trapped particle, we chose the two differently doped samples to present distinct  
10 light-to-heat conversion efficiencies (see Methods and Supporting Information for details).  
11 The excitation of  $\text{NaYbF}_4:\text{Er}^{3+},\text{Nd}^{3+}$  microcrystals by 788 nm radiation produces an increase  
12 in their internal temperature. This is evidenced in Figure 1(c) where a clear change of the  
13 relative intensity of the highlighted bands takes place when laser power is increased. On the  
14 other hand, no temperature increase with laser power is seen for  $\text{NaYF}_4:\text{Er}^{3+},\text{Yb}^{3+}$  UCPs  
15 (see Figure 1(d)) which have lower absorption.

16 Both samples are positive uniaxial birefringent crystals, where the optical axis is perpen-  
17 dicular to the two hexagonal facets.<sup>19,20</sup> Thus these particles can be rotated by a circularly  
18 polarized (CP) beam. In addition, both types of particles are non-spherical. This affects the  
19 trapping properties of the particle. Due to the action of two different optical torques, the  
20 particle is stably trapped with its optical axis parallel to the polarization of the trapping  
21 laser, if linearly polarized (LP) light is used.<sup>20</sup> Thus, the trapped particle is stably orientated  
22 with its longitudinal axis parallel to the propagation direction of the trapping beam. This  
23 means that, when CP light is used, the rotation axis is parallel to the longitudinal axis of  
24 the particle.

25  
26  
27  
28  
29  
30  
31  
32  
33  
34  
35  
36  
37  
38  
39  
40  
41  
42  
43  
44  
45  
46  
47  
48 **Thermometric techniques.** The following described techniques (luminescence, rotation  
49 rate and trap stiffness methods) can provide a value for the thermal loading ( $C_P$ ), which is the  
50 temperature increment per unit of power generated by the trapped particle. The temperature  
51 increase depends on the amount of light absorbed by the particle and the fraction of that light  
52  
53  
54  
55  
56  
57  
58  
59  
60

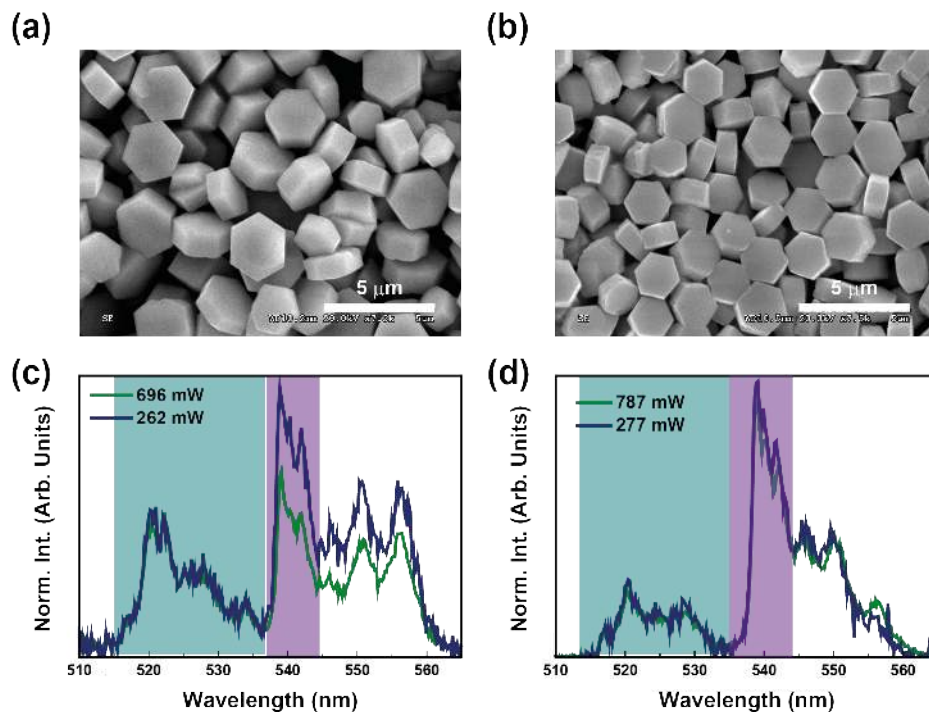


Figure 1: SEM images of (a) NaYbF<sub>4</sub>:Er<sup>3+</sup>,Nd<sup>3+</sup> and (b) NaYF<sub>4</sub>:Er<sup>3+</sup>,Yb<sup>3+</sup> particles and their corresponding luminescence spectra in (c) and (d), respectively, for two different excitation powers.

that is converted into heat through energy dissipation processes (see Supporting Information for details). Although both the absorption rate and energy dissipation are expected to depend on temperature, this dependence has been shown to be negligible in previous studies which show a linear temperature increment with laser power in the range of temperature explored here.<sup>12</sup> Thus we assume a temperature increment ( $T$ ) with the laser power ( $P$ ) of the form:  $T(P) = T_0 + C_P P$ , where  $T_0$  is the initial temperature with no laser power applied (i.e. room temperature). We stress that the rotation rate and trap stiffness methods described below are independent of particle size and shape distinguishing this approach from previous, established routes for determination of CoM temperature.<sup>10,14,15,21</sup>

*Luminescence method.* This method obtains a value of the thermal loading ( $C_{PI}$ ) from the changes in the intensity ratio ( $\frac{I_2}{I_1}$ ) of the two temperature-dependent emission bands:

$$\ln\left(\frac{I_2}{I_1}\right) = -C_E \frac{1}{T_0 + C_{PI}P} + C_I, \quad (1)$$

where  $C_E$  and  $C_I$  are constants which include information of the thermalized energy levels involved in the radiative transitions (see Supporting Information for details).<sup>8,17</sup> Thus,  $C_{PI}$  can be determined from the evolution of  $\ln(I_2/I_1)$  with  $P$ . It is worthy of note that, contrary to conventional thermometry studies, a prior calibration of the luminescence response with temperature is not needed since that information is included in the fitting parameters  $C_E$  and  $C_I$ .

*Rotation rate method.* When a birefringent particle is trapped by a CP beam, an optical torque will act on it:  $\tau_{opt} = \Delta\sigma P/\omega$ , where  $\Delta\sigma$  is the change in the degree of polarization and  $\omega$  the angular frequency of light. The magnitude of  $\tau_{opt}$  depends on the birefringence of the particle, which induces a phase retardation in the components of the CP light resulting in a change in the output polarization. In addition, optical torque transfer can be produced through absorption of the CP light by the particle.<sup>22</sup> Due to the Stokes drag torque counteracting  $\tau_{opt}$ , the trapped particle rotates at a terminal rotation rate:  $\Omega = (\Delta\sigma P)/(\beta(\eta)\omega)$ , where  $\beta(\eta)$  denotes the rotational Stokes drag coefficient, which is dependent on the medium's viscosity ( $\eta(T)$ ). Here we have used a tabulated dataset<sup>23</sup> to obtain the temperature-dependent viscosity of water:  $\eta(T) = A + Be^{-T/C}$ , with  $A = 0.156 \pm 0.007$  mPas,  $B = 1.37 \pm 0.02$  mPas and  $C = 41 \pm 1$  °C. Therefore the dependence of  $\Omega(P)$  can be written in the form:

$$\Omega(P) = \frac{C_R P}{A + Be^{-(T_0 + C_{P\Omega}P)/C}}, \quad (2)$$

where  $C_R = \Delta\sigma/(\omega\beta')$ , with  $\beta' = \beta/\eta$ , is a constant that includes the characteristics of the particle and  $\tau_{opt}$ . The linear dependence of  $T$  with the laser power has also been included. The thermal loading ( $C_{P\Omega}$ ) can be determined from the fitting of Eq.(2) to the experimental rotation rate as a function of the laser power. Therefore, here,  $C_{P\Omega}$  can be directly obtained from  $\Omega(P)$ , while traditional studies require a prior knowledge of the drag coefficient of the



1  
2  
3 particle (and therefore particle's size and shape) and the thermal profile in the surrounding  
4 medium in order to be able to fit the measured rotation rate to the theoretical model.<sup>21,24</sup>  
5  
6 In our case, particle's size and shape are included as the fitting parameter  $C_R$ .  
7  
8  
9

10 *Trap stiffness method.* A particle trapped in an optical potential undergoes Brownian mo-  
11 tion subject to the trap stiffness, which can be obtained by the analysis of its position power  
12 spectrum.<sup>25</sup> The corner frequency ( $f_c$ ) of the power spectrum determines the trap stiffness:  
13  $\kappa = 2\pi f_c \beta(T)$ , which is also dependent on  $T$ <sup>21,26</sup> and therefore provides a way to measure  
14 temperature. Correct determination of the trap stiffness requires knowledge of the thermal  
15 loading ( $C_{P\kappa}$ ). We determine its value by a numerical optimization routine which enforces  
16 the expected linear relationship between  $\kappa$  and  $P$  (see Supporting Information for details).  
17 This novel method presents several advantages in contrast to the traditional ways used to  
18 measure temperature from the particle's Brownian motion. Usually, power spectrum and  
19 equipartition method results are combined.<sup>15</sup> However, former studies have shown that dif-  
20 ferent trap stiffness calibration methods lead to a different value of the trap stiffness due  
21 to their particular limitations,<sup>27</sup> and therefore, the combination of results from different  
22 methods introduces more uncertainty in the measurement of the temperature. Moreover, to  
23 obtain a value of  $\kappa$  from the equipartition method, the QPD signal needs to be converted  
24 to displacement in distance units, rather than voltage, thus a calibration is needed.<sup>13</sup> In  
25 addition, to obtain a value of  $\kappa$  from the power spectrum, a knowledge of the drag coefficient  
26 of the particle (including size and shape) is required. In this case, we have used a theoretical  
27 translational drag coefficient for the disc-like particles:  $\beta' = \beta/\eta = 6Vf/f_0R^{-2}$ , where  $V$   
28 and  $R$  are the volume and radius of the particle, respectively, and  $f/f_0$  the Perrin friction  
29 factor.<sup>28</sup> Nevertheless, this information is not necessary in our case since our procedure can  
30 be applied for a normalized value of  $\kappa$  ( $\kappa/2\pi\beta' = f_c\eta$ ), since the drag coefficient is a constant  
31 that multiplies the viscosity of the medium.  
32  
33  
34  
35  
36  
37  
38  
39  
40  
41  
42  
43  
44  
45  
46  
47  
48  
49  
50  
51  
52  
53  
54  
55  
56  
57  
58  
59  
60

## Results and discussion

**Highly-absorbing particles.** Figures 2(a-c) show the experimental data obtained from an optically trapped  $\text{NaYbF}_4:\text{Er}^{3+},\text{Nd}^{3+}$  microparticle for the different techniques. The change in the intensity ratio with the laser power (Figure 2(a)) indicates an increment of the temperature of the particle according to a thermal loading of  $C_{PI} = 0.37 \pm 0.06 \text{ }^\circ\text{CmW}^{-1}$ . Figure 2(b) shows the rotation rate as a function of the applied laser power. The best fit of the experimental data with Eq. (2) provides a thermal loading of  $C_{P\Omega} = 0.35 \pm 0.05 \text{ }^\circ\text{CmW}^{-1}$ . Finally, Figure 2(c) shows a superlinear behavior of  $\kappa$ , assuming a constant temperature ( $T = 22 \text{ }^\circ\text{C}$ ) (green circles). The green line is a guide for the eye. Blue data correspond to the optimized linear relationship between  $\kappa$  and  $P$  for a thermal loading of  $C_{P\kappa} = 0.11 \pm 0.04 \text{ }^\circ\text{CmW}^{-1}$ . All the results are summarized in Table 1.

These thermal loadings of a single  $\text{NaYbF}_4:\text{Er}^{3+},\text{Nd}^{3+}$  particle are one order of magnitude larger than those measured for colloidal solutions of Nd-doped nanoparticles,<sup>12</sup> but they are comparable to those reported for individual gold nanoparticles.<sup>26,29</sup> This suggests high light-to-heat conversion efficiency of the studied particles (see Supporting Information for details). Due to this fact, temperatures above the boiling point of water were reached during experiments, as shown in Figure 3. We note that there are a number of reports showing light-excited particles exceeding the boiling point of water at the standard pressure.<sup>29-31</sup> However, it is often the case that no bubble formation was observed probably due to the increase of the critical temperature in the proximity of the particle (see Supporting Information for details). In addition, it is worth noting that no signs of particle disruption were observed even though its temperature can reach as high as  $280 \text{ }^\circ\text{C}$  during the trapping experiments (see Supporting Information for details).

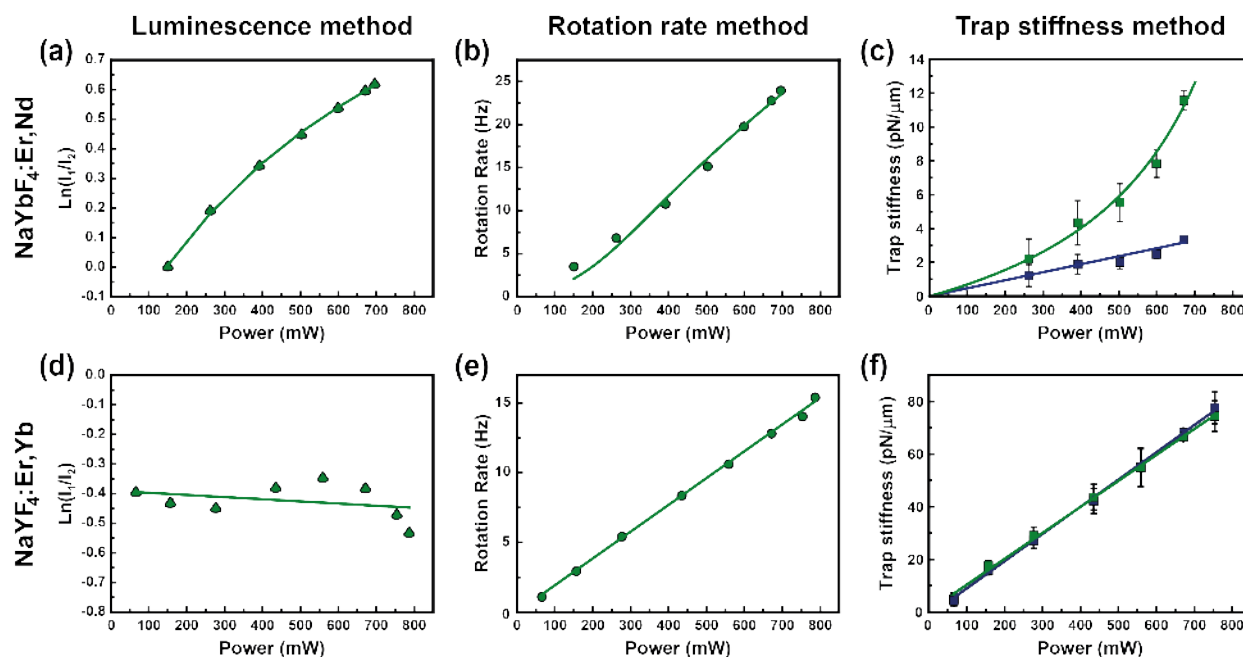


Figure 2: (a) Change in the intensity ratio as a function of the trapping power, (b) rotation rate as a function of the laser power and (c) trap stiffness as a function of the laser power when temperature is set to 22 °C (green) and when temperature increment is considered (blue) for a NaYbF<sub>4</sub>:Er<sup>3+</sup>,Nd<sup>3+</sup> microparticle. (d) Change in the intensity ratio as a function of the trapping power,(e) rotation rate as a function of the laser power and (f) trap stiffness as a function of the laser power when temperature is set to 22 °C (green) and when temperature increment is consider (blue) for a NaYF<sub>4</sub>:Er<sup>3+</sup>,Yb<sup>3+</sup> microparticle. Where not present, error bars are smaller than the symbols denoting the data points.

Table 1: Measured thermal loadings. <sup>a</sup>This thermal loading was calculated from the luminescence thermal resolution (0.5 °C) divided by the maximum applied laser power (~ 800 mW). All values are given in °CmW<sup>-1</sup>.

Particle	NaYbF <sub>4</sub> :Er <sup>3+</sup> ,Nd <sup>3+</sup>	NaYF <sub>4</sub> :Er <sup>3+</sup> ,Yb <sup>3+</sup>
Luminescence	0.37 ± 0.06	< 0.001 <sup>a</sup>
Rotation rate	0.35 ± 0.05	0.001 <sup>+0.006</sup> <sub>-0.001</sub>
Trap stiffness	0.11 ± 0.04	0.007 ± 0.003

**Weakly-absorbing particles.** The temperature increment produced by a optically trapped single NaYF<sub>4</sub>:Er<sup>3+</sup>,Yb<sup>3+</sup> microparticle was also measured which is a particle with a lower absorption at 788 nm than NaYbF<sub>4</sub>:Er<sup>3+</sup>,Nd<sup>3+</sup> particles. Results are shown in Figures 2(d-f) and Table 1. The thermal loading for the luminescence method could not be calculated because the temperature increment by the laser-induced heating is lower than the thermal resolution of the technique, as explained in the next section. The rotation rate analysis

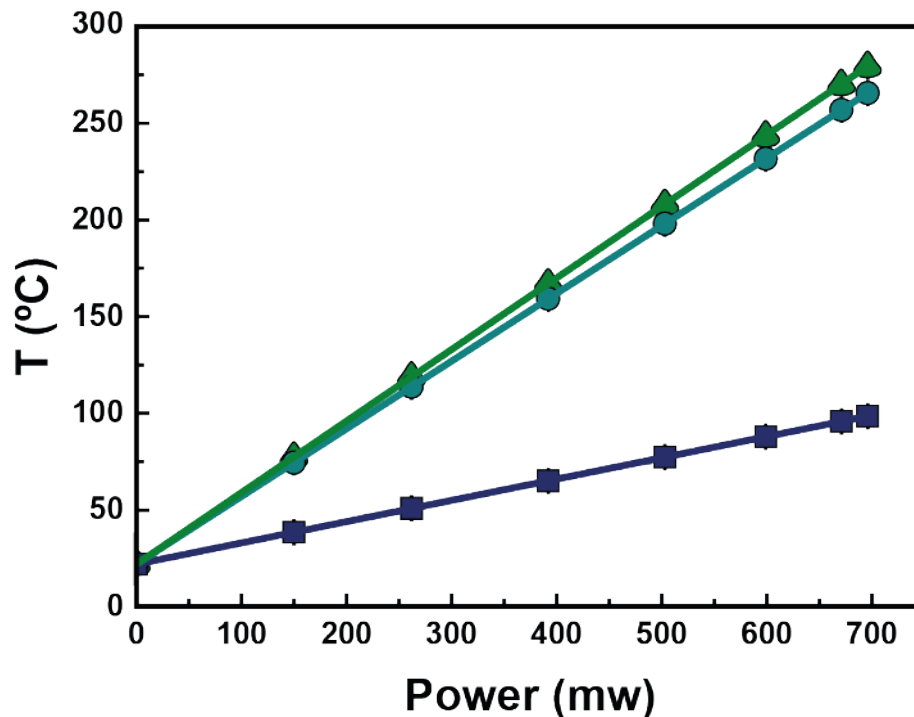


Figure 3: Temperature as a function of power measured for a  $\text{NaYbF}_4:\text{Er}^{3+},\text{Nd}^{3+}$  microparticle by using the three thermometric methods: luminescence (green triangles), rotation rate (cyan circles), trap stiffness (navy squares). A room temperature of  $22^\circ\text{C}$  is assumed.

provides a thermal loading value that agrees with that estimated from luminescence thermometry. On the other hand, the trap stiffness measurements give a non-negligible thermal loading that deviates by an order of magnitude (see Table 1). This discrepancy could result from the fact that the trap stiffness method is very sensitive to the accuracy in the determination of  $f_c$ . Therefore, even in the absence of a temperature increment, the linearity of  $\kappa$  can be affected by the uncertainty in the measurement of  $f_c$ , and the optimization process is able to find a value of  $C_{P\kappa}$  which enhances the linear relationship between  $\kappa$  and  $P$ .

We note that the results obtained for a non-heated  $\text{NaYF}_4:\text{Er}^{3+},\text{Yb}^{3+}$  microparticle evidence that the main heating source in the experiments developed with a  $\text{NaYbF}_4:\text{Er}^{3+},\text{Nd}^{3+}$  microcrystal is the particle itself. Water presents a low absorption coefficient ( $\alpha_{\text{abs}} = 0.02 \text{ cm}^{-132}$ ) at 790 nm, which is negligible in the present regime.

It is worth noticing that Figure 2 shows that  $\text{NaYF}_4:\text{Er}^{3+},\text{Yb}^{3+}$  microparticles present larger trap stiffness and a lower rotation rate than  $\text{NaYbF}_4:\text{Er}^{3+},\text{Nd}^{3+}$  microcrystals. We

1  
2  
3 attribute this discrepancy to the different temperatures and absorption coefficients of the  
4 particles. In the case of the rotational motion, the temperature increment produces a re-  
5 duction in the viscosity of the surrounding medium leading to a larger rotation rate for the  
6 NaYbF<sub>4</sub>:Er<sup>3+</sup>,Nd<sup>3+</sup> microparticles. In addition, optical torque can be transferred through  
7 absorption producing an increase in the rotation rate for the highly-absorbing particles. The  
8 contrary effect is observed for the trap stiffness which is not only reduced as a result of the  
9 increment in the temperature, but also due to the larger absorption of the particles which  
10 increases the scattering force. Consequently, NaYbF<sub>4</sub>:Er<sup>3+</sup>,Nd<sup>3+</sup> microparticles are trapped  
11 in a weaker optical potential region which leads to a reduction in the trap stiffness.  
12  
13  
14  
15  
16  
17  
18  
19  
20  
21

22 **Thermal sensitivity and resolution.** The thermal sensitivity ( $S$ ) is used to describe  
23 and compare the performance of different thermometric systems:  $S = \frac{1}{C} \frac{dC}{dT}$ , where  $C$  is the  
24 parameter used to determine the changes in the temperature, i.e. intensity ratio ( $\frac{I_1}{I_2}$ ), trap  
25 stiffness ( $\kappa$ ) or rotation rate ( $\Omega$ ). Since both rotation rate and trap stiffness methods measure  
26 the changes in temperature through the viscosity of the surrounding medium, they present  
27 the same sensitivity ( $2.0\%K^{-1}$ ), which is three times larger than that of the luminescence  
28 method ( $0.66\%K^{-1}$ ). This latter case is within the range published for similar luminescence  
29 thermometers ( $0.2 - 2.3\%K^{-1}$ ).<sup>8</sup>  
30  
31  
32  
33  
34  
35  
36  
37

38 These thermal sensitivities can be used to obtain a value of the thermal resolution ( $\delta T$ )  
39 of each technique:  $\delta T = \frac{1}{S} \frac{\delta C}{C}$ , where  $\delta C$  is the uncertainty in the determination of the pa-  
40 rameter  $C$ . The thermal resolutions are  $0.5^\circ C$ ,  $0.03^\circ C$ , and  $0.1^\circ C$  for the luminescence,  
41 rotation rate, and trap stiffness measurements, respectively. Here, the thermal resolution of  
42 the luminescence method was used to estimate the internal thermal loading (see **Table 1**) for  
43 the weakly-absorbing particle. The thermal resolution achieved by the combined methods  
44 ensures a higher accuracy in the determination of the thermal changes than previously pub-  
45 lished studies of optically heated or cooled particles in aqueous media.<sup>14-16</sup> This capability  
46 will improve future analysis of the CoM and internal temperatures and their coupling.  
47  
48  
49  
50  
51  
52  
53  
54  
55  
56  
57  
58  
59  
60

1  
2  
3 **Different degrees of freedom.** Furthermore, this tripartite approach allows us for the  
4 first time to simultaneously analyze the temperatures obtained from three different degrees  
5 of freedom of the particle: *internal*, *rotational* and *translational*. We note that it has been  
6 suggested, both experimentally and theoretically, by previous studies that the medium tem-  
7 perature probed by the dynamics of a particle can yield different temperature depending  
8 on whether the rotational or translational motion is considered.<sup>15,21</sup> Moreover, the inter-  
9 nal temperature of the particle is typically higher than the temperature of the surrounding  
10 medium.  
11

12  
13 In the case of highly-absorbing particles ( $\text{NaYbF}_4:\text{Er}^{3+},\text{Nd}^{3+}$ ), Table 1 shows that the ther-  
14 mal loading measured from the luminescence and the rotation methods are in good agreement  
15 within the experimental error, whereas the trap stiffness method exhibits a lower temper-  
16 ature (see also Figure 3). This discrepancy can be tentatively explained by taking into  
17 account that the temperature of the fluid varies with the distance from the particle surface,  
18 which means that there will be a non-uniform distribution of fluid viscosity around the par-  
19 ticle. As mentioned above, previous studies suggest that the particle experiences a different  
20 temperature depending on whether we consider rotational or translational motion, which  
21 is known as "hot Brownian motion" (HBM).<sup>15,33-35</sup> Therefore, this non-equilibrium steady  
22 state affects the Brownian dynamics of the particle depending upon whether the rotational or  
23 translational degree of freedom is under consideration.<sup>15,21,34,35</sup> When rotating, the particle  
24 dynamics are affected by the liquid in close proximity to it which is at a temperature close to  
25 its internal, whereas when it translates the particle explores regions at a lower temperature.  
26 In other words, the fluid velocity field is more localized near the particle for rotation than for  
27 translation, therefore the effective temperature for rotational motion is higher than for trans-  
28 lational motion.<sup>35</sup> This thermal difference between the translational and rotational degrees  
29 of freedom would be enhanced for larger temperature increments and in media with a lower  
30 heat conductivity (such as low pressure gas or vacuum) where heat dissipation is reduced.<sup>4,13</sup>  
31 Even though former studies have shown consistent results with those presented here, there  
32  
33  
34  
35  
36  
37  
38  
39  
40  
41  
42  
43  
44  
45  
46  
47  
48  
49  
50  
51  
52  
53  
54  
55  
56  
57  
58  
59  
60

1  
2  
3 is not a clear explanation of the discrepancy between the different degrees of freedom. The  
4 technique here presented can be used in future studies on the dynamics of optically trapped  
5 particles in HBM conditions to give a better insight of the problem in different media.  
6  
7

8  
9 Finally, our results show that the temperature of the internal degree of freedom can only  
10 be assessed by using the luminescence of the particle. The rotational degree of freedom  
11 is affected by the superficial temperature of the particle which is, under our experimental  
12 uncertainty, equal to that of the internal degree of freedom. On the other hand, the trans-  
13 lational degree of freedom exhibits a lower temperature than that of the particle itself due  
14 to the HBM. Our study shows that, in non-equilibrium thermal conditions, the Brownian  
15 dynamics, i.e. the external degrees of freedom, of the particle do not give a real value of  
16 the particle temperature, whereas only the luminescence, i.e. the internal degree of freedom,  
17 allows an access to the internal temperature of the particle.  
18  
19  
20  
21  
22  
23  
24  
25  
26  
27  
28

## 29 Conclusions

30  
31  
32 In summary, the temperature of an optically trapped upconverting particle has been mea-  
33 sured by studying its internal and external degrees of freedom. The internal degree of freedom  
34 has been experimentally assessed through the temperature-dependent luminescence of the  
35 particle, while the rotational and translational degrees of freedom were analyzed through  
36 the rotation rate and the trap stiffness of the particle, respectively. The higher thermal  
37 resolution in comparison with former studies has allowed a detailed study between these  
38 three independent methods. Both the internal and rotational degrees of freedom yielded the  
39 same effective temperature, while the translational motion exhibited a lower temperature in  
40 the non-thermal equilibrium state. These results are in good agreement with the hot Brow-  
41 nian motion to which the particle is subjected. Moreover, we note that any non-spherical  
42 particle will present non-zero off-diagonal terms in its hydrodynamic friction tensor that  
43 couples translational and rotational motion.<sup>36</sup> This is a minor effect not considered in the  
44  
45  
46  
47  
48  
49  
50  
51  
52  
53  
54  
55  
56  
57  
58  
59  
60

1  
2  
3 study, however optical forces and torques acting on the particles may be modified by this  
4 hydrodynamic coupling. Follow up work would give a better insight in this matter.  
5  
6

7 The tripartite thermometric method described here does not require any knowledge of  
8 the particle characteristics or any previous calibration, which enhanced thermal sensitivity  
9 and resolution. This is a key advantage in comparison to former studies where theoretical  
10 assumptions and additional particle size and shape information are required for the deter-  
11 mination of temperature, which may increase the measurement uncertainty. Thus, it would  
12 be very interesting to show further studies of particles with different size, shape and internal  
13 structure in a distinct solvent to corroborate the wide applicability of the technique. Further-  
14 more, upconverting particles can offer a multitude of opportunities in different fields such as  
15 quantum optics, levitated-optomechanics and a wide range of biological studies. Thus, our  
16 method will interest a broad audience working on areas in the determination and control of  
17 temperature at the micro and nanoscale.  
18  
19  
20  
21  
22  
23  
24  
25  
26  
27  
28  
29  
30

## 31 **Methods and materials**

  
32  
33

34 **Particle preparation.** The hydrothermal procedure used to synthesize the two different  
35 types UCPs is described elsewhere.<sup>9,10</sup> The first sample is composed of colloidal NaYbF<sub>4</sub>  
36 microcrystals, doped with a 2 % of trivalent erbium and a 10 % of trivalent neodymium ions,  
37 while the other is a colloidal solution of NaYF<sub>4</sub>:0.5%Er<sup>3+</sup>,5%Yb<sup>3+</sup> microcrystals.  
38  
39  
40  
41  
42  
43

44 **Optical trapping set-up.** We use a standard optical tweezers set-up with a Ti:Sapphire  
45 laser (Coherent, Mira 900-F) tuned to a wavelength of 788 nm. This wavelength is chosen  
46 because it is able to both excite the UC luminescence and induce absorption within the  
47 trapped particle, while minimizing any absorption by water. The LP beam was focused by  
48 a high numerical aperture (NA) microscope objective lens (Nikon, E Plan, 100× NA=1.25,  
49 in oil) to trap individual particles suspended in deionized water. A quarter-wave plate was  
50 placed immediately before the microscope objective in order to switch the beam's polarization  
51  
52  
53  
54  
55  
56  
57  
58  
59  
60



1  
2  
3 from LP to CP or vice versa. For the analysis of the particle dynamics, the forward scattered  
4 light by the trapped particle was collected using a condenser lens (Mituyoto, M Plan Apo,  
5  $20\times$  NA = 0.42) and detected by a quadrant photodiode (QPD, First Sensor, QP50-6SD2,-3  
6 dB at 150 kHz). A CCD camera (Basler, piA640-210gm) was used for the visualization of the  
7 trapped particle. Finally, a compact, fiber-coupled spectrometer (Oceanoptics, USB4000)  
8 was used for the analysis of the particle's luminescence. The very same condenser lens was  
9 used to collect the luminescence and a shortpass filter (Thorlabs, FESH0700) was placed at  
10 the entrance of the fiber to block the laser light from reaching the detector.  
11  
12  
13  
14  
15  
16  
17  
18  
19

20 **Experimental protocol.** The following procedure was applied for the determination of  
21 the thermal loading through the developed tripartite thermometric technique. First, the  
22 trapped particle was set into rotation by a CP beam at different excitation powers up to  
23 800 mW. At each power, a rotation signal was recorded by the QPD for 6 min. During that  
24 time, six luminescence spectra were measured every 1 min. Once the rotation experiment was  
25 completed, the *same* particle was trapped by an LP beam to measure the trap stiffness for the  
26 same power range using the QPD. At each power level, ten consecutive measurements were  
27 performed in order to obtain reliable statistics, together with six consecutive measurements  
28 of luminescence spectra following the trap stiffness measurement.  
29  
30  
31  
32  
33  
34  
35  
36  
37  
38  
39

## 40 **Author information**

41 P.R.S. and Y.A. performed the experiments and data analysis. All authors contributed to the  
42 development and planning of the project, interpretation and discussion of the data. P.R.S.,  
43 Y.A. and K.D. wrote the manuscript. K.D. supervised the project. The authors declare no  
44 competing financial interests.  
45  
46  
47  
48  
49  
50  
51  
52  
53  
54  
55  
56  
57  
58  
59  
60

## Acknowledgement

P.R.S thanks the Spanish Ministerio de Economía y Competitividad (MINECO) for the “Promoción del talento y su Empleabilidad en I+D+i” state program for funding. We thank the UK Engineering and Physical Sciences Research Council for funding through grant EP/P030017/1 and MINECO for funding through grant MAT2016-75362-C3-1-R. COST Action CM1403 and UAM-Santander Yerun Projects are also acknowledged. This work was also Supported by Comunidad Autónoma de Madrid (B2017/BMD-3867RENIM-CM), by the European Commission (NanoTBTech). Work co-financed by European Structural and Investment Fund. Graham D. Bruce is acknowledge for technical support.

## Supporting Information Available

The following file is available free of charge.

- Supp.pdf: Supporting information

This material is available free of charge via the Internet at <http://pubs.acs.org/>.

## References

- (1) Li, T.; Kheifets, S.; Raizen, M. G. Millikelvin cooling of an optically trapped microsphere in vacuum. *Nature Physics* **2011**, *7*, 527.
- (2) Li, Y. L.; Millen, J.; Barker, P. F. Cooling the centre-of-mass motion of a silica microsphere. *Proc. SPIE, Optical Trapping and Optical Micromanipulation XI* **2014**, *9164*, 916404.
- (3) Bullier, N. P.; Pontin, A.; Barker, P. F. Millikelvin cooling of the center-of-mass motion of a levitated nanoparticle. *Proc. SPIE, Optical Trapping and Optical Micromanipulation XIV* **2017**, *10347*, 103471K.

- 1  
2  
3 (4) Hebestreit, E.; Reimann, R.; Frimmer, M.; Novotny, L. Measuring the internal temper-  
4 ature of a levitated nanoparticle in high vacuum. *Physical Review A* **2018**, *97*, 043803.  
5  
6
- 7  
8 (5) Dong, H.; Sun, L.-D.; Yan, C.-H. Basic understanding of the lanthanide related upcon-  
9 version emissions. *Nanoscale* **2013**, *5*, 5703–5714.  
10  
11
- 12  
13 (6) Zhou, B.; Shi, B.; Jin, D.; Liu, X. Controlling upconversion nanocrystals for emerging  
14 applications. *Nat Nano* **2015**, *10*, 924–936.  
15  
16
- 17  
18 (7) Nadort, A.; Zhao, J.; Goldys, E. M. Lanthanide upconversion luminescence at the  
19 nanoscale: fundamentals and optical properties. *Nanoscale* **2016**, *8*, 13099–13130.  
20  
21
- 22  
23 (8) Jaque, D.; Vetrone, F. Luminescence nanothermometry. *Nanoscale* **2012**, *4*, 4301–4326.  
24  
25
- 26  
27 (9) Rodríguez-Sevilla, P.; Zhang, Y.; Haro-González, P.; Sanz-Rodríguez, F.; Jaque, F.;  
28 Solé, J. G.; Liu, X.; Jaque, D. Thermal Scanning at the Cellular Level by an Optically  
29 Trapped Upconverting Fluorescent Particle. *Advanced Materials* **2016**, *28*, 2421–2426.  
30  
31
- 32  
33 (10) Rodríguez-Sevilla, P.; Lee, T.; Liang, L.; Haro-González, P.; Lifante, G.; Liu, X.;  
34 Jaque, D. Light-Activated Upconverting Spinners. *Advanced Optical Materials* **2018**,  
35 1800161.  
36  
37
- 38  
39 (11) Rahman, A. T. M. A.; Barker, P. F. Laser refrigeration, alignment and rotation of  
40 levitated  $\text{Yb}^{3+}$ :YLF nanocrystals. *Nature Photonics* **2017**, *11*, 634–638.  
41  
42
- 43  
44 (12) Ximendes, E. C.; Rocha, U.; Jacinto, C.; Kumar, K. U.; Bravo, D.; Lopez, F. J.;  
45 Rodriguez, E. M.; Garcia-Sole, J.; Jaque, D. Self-monitored photothermal nanoparticles  
46 based on core-shell engineering. *Nanoscale* **2016**, *8*, 3057–3066.  
47  
48
- 49  
50 (13) Millen, J.; Deesuwan, T.; Barker, P.; Anders, J. Nanoscale temperature measurements  
51 using non-equilibrium Brownian dynamics of a levitated nanosphere. *Nature Nanotech-*  
52 *nology* **2014**, *9*, 425.  
53  
54  
55  
56  
57  
58  
59  
60

- 1  
2  
3 (14) Roder, P. B.; Smith, B. E.; Zhou, X.; Crane, M. J.; Pauzauskie, P. J. Laser refrigera-  
4 tion of hydrothermal nanocrystals in physiological media. *Proceedings of the National*  
5 *Academy of Sciences* **2015**, *112*, 15024–15029.  
6  
7  
8  
9  
10 (15) Hajizadeh, F.; Shao, L.; Andrén, D.; Johansson, P.; Rubinsztein-Dunlop, H.; Käll, M.  
11 Brownian fluctuations of an optically rotated nanorod. *Optica* **2017**, *4*, 746–751.  
12  
13  
14 (16) Zhou, X.; Smith, B. E.; Roder, P. B.; Pauzauskie, P. J. Laser Refrigeration of  
15 Ytterbium-Doped Sodium-Yttrium-Fluoride Nanowires. *Advanced Materials* **2016**, *28*,  
16 8658–8662.  
17  
18  
19  
20  
21 (17) Zhou, S. S.; Deng, K. M.; Wei, X. T.; Jiang, G. C.; Duan, C. K.; Chen, Y. H.; Yin, M.  
22 Upconversion luminescence of NaYF<sub>4</sub>: Yb<sup>3+</sup>, Er<sup>3+</sup> for temperature sensing. *Opt. Com-*  
23 *mun.* **2013**, *291*, 138–142.  
24  
25  
26  
27  
28 (18) Baral, S.; Johnson, S. C.; Alaulamie, A. A.; Richardson, H. H. Nanothermometry using  
29 optically trapped erbium oxide nanoparticle. *Appl. Phys. A* **2016**, *122*, 1–8.  
30  
31  
32  
33 (19) Chen, P.; Song, M.; Wu, E.; Wu, B.; Zhou, J.; Zeng, H.; Liu, X.; Qiu, J. Polariza-  
34 tion modulated upconversion luminescence: single particle vs. few-particle aggregates.  
35 *Nanoscale* **2015**, *7*, 6462–6466.  
36  
37  
38  
39  
40 (20) Rodríguez-Sevilla, P.; Zhang, Y.; de Sousa, N.; Marqués, M. I.; Sanz-Rodríguez, F.;  
41 Jaque, D.; Liu, X.; Haro-González, P. Optical Torques on Upconverting Particles for  
42 Intracellular Microrheometry. *Nano Letters* **2016**, *16*, 8005–8014.  
43  
44  
45  
46  
47 (21) Arita, Y.; Richards, J. M.; Mazilu, M.; Spalding, G. C.; Skelton Spesyvtseva, S. E.;  
48 Craig, D.; Dholakia, K. Rotational Dynamics and Heating of Trapped Nanovaterite  
49 Particles. *ACS Nano* **2016**, *10*, 11505–11510.  
50  
51  
52  
53  
54 (22) Friese, M. E. J.; Enger, J.; Rubinsztein-Dunlop, H.; Heckenberg, N. R. Optical angular-  
55  
56  
57  
58  
59  
60

- 1  
2  
3 momentum transfer to trapped absorbing particles. *Physical Review A* **1996**, *54*, 1593–  
4 1596.  
5  
6  
7
- 8 (23) Kestin, J.; Sokolov, M.; Wakeham, W. A. Viscosity of liquid water in the range  $-8^{\circ}\text{C}$   
9 to  $150^{\circ}\text{C}$ . *J. Phys. Chem. Ref. Data* **1978**, *7*, 941–948.  
10  
11  
12
- 13 (24) Parkin, S. J.; KnÄner, G.; Nieminen, T. A.; Heckenberg, N. R.; Rubinsztein-  
14 Dunlop, H. Picoliter viscometry using optically rotated particles. *Physical Review E*  
15 **2007**, *76*, 041507.  
16  
17  
18
- 19 (25) Berg-Sørensen, K.; Flyvbjerg, H. Power spectrum analysis for optical tweezers. *Review*  
20 *of Scientific Instruments* **2004**, *75*, 594–612.  
21  
22  
23
- 24 (26) Seol, Y.; Carpenter, A. E.; Perkins, T. T. Gold nanoparticles: enhanced optical trapping  
25 and sensitivity coupled with significant heating. *Opt. Lett.* **2006**, *31*, 2429–2431.  
26  
27  
28
- 29 (27) Sarshar, M.; Wong, W. T.; Anvari, B. Comparative study of methods to calibrate the  
30 stiffness of a single-beam gradient-force optical tweezers over various laser trapping  
31 powers. *Journal of Biomedical Optics* **2014**, *19*.  
32  
33  
34  
35
- 36 (28) Erb, R. M.; Segmehl, J.; Charilaou, M.; Löffler, J. F.; Studart, A. R. Non-linear align-  
37 ment dynamics in suspensions of platelets under rotating magnetic fields. *Soft Matter*  
38 **2012**, *8*, 7604–7609.  
39  
40  
41  
42
- 43 (29) Kyrsting, A.; Bendix, P. M.; Stamou, D. G.; Oddershede, L. B. Heat Profiling of Three-  
44 Dimensionally Optically Trapped Gold Nanoparticles using Vesicle Cargo Release. *Nano*  
45 *Lett.* **2011**, *11*, 888–892.  
46  
47  
48  
49
- 50 (30) Lehmuskero, A.; Ogier, R.; Gschneidtnr, T.; Johansson, P.; Käll, M. Ultrafast Spinning  
51 of Gold Nanoparticles in Water Using Circularly Polarized Light. *Nano Letters* **2013**,  
52 *13*, 3129–3134.  
53  
54  
55  
56  
57  
58  
59  
60

- 1  
2  
3 (31) Baffou, G.; Polleux, J.; Rigneault, H.; Monneret, S. Super-Heating and Micro-Bubble  
4 Generation around Plasmonic Nanoparticles under cw Illumination. *The Journal of*  
5 *Physical Chemistry C* **2014**, *118*, 4890–4898.  
6  
7  
8  
9  
10 (32) Kedenburg, S.; Vieweg, M.; Gissibl, T.; Giessen, H. Linear refractive index and absorp-  
11 tion measurements of nonlinear optical liquids in the visible and near-infrared spectral  
12 region. *Opt. Mater. Express* **2012**, *2*, 1588–1611.  
13  
14  
15  
16 (33) Rings, D.; Schachoff, R.; Selmke, M.; Cichos, F.; Kroy, K. Hot Brownian Motion.  
17 *Physical Review Letters* **2010**, *105*, 090604.  
18  
19  
20  
21 (34) Ruijgrok, P. V.; Verhart, N. R.; Zijlstra, P.; Tchebotareva, A. L.; Orrit, M. Brown-  
22 ian Fluctuations and Heating of an Optically Aligned Gold Nanorod. *Physical Review*  
23 *Letters* **2011**, *107*, 037401.  
24  
25  
26  
27 (35) Rings, D.; Chakraborty, D.; Kroy, K. Rotational hot Brownian motion. *New Journal*  
28 *of Physics* **2012**, *14*, 053012.  
29  
30  
31  
32 (36) Kraft, D. J.; Wittkowski, R.; ten Hagen, B.; Edmond, K. V.; Pine, D. J.; LÄűwen, H.  
33 Brownian motion and the hydrodynamic friction tensor for colloidal particles of complex  
34 shape. *Physical Review E* **2013**, *88*, 050301.  
35  
36  
37  
38  
39  
40  
41  
42  
43  
44  
45  
46  
47  
48  
49  
50  
51  
52  
53  
54  
55  
56  
57  
58  
59  
60

1  
2  
3 Figure 1: SEM images of (a)  $\text{NaYbF}_4:\text{Er}^{3+},\text{Nd}^{3+}$  and (b)  $\text{NaYF}_4:\text{Er}^{3+},\text{Yb}^{3+}$  particles and  
4 their corresponding luminescence spectra in (c) and (d), respectively, for two different exci-  
5 tation powers.  
6  
7  
8  
9

10 Figure 2: (a) Change in the intensity ratio as a function of the trapping power, (b) rotation  
11 rate as a function of the laser power and (c) trap stiffness as a function of the laser power  
12 when temperature is set to  $22^\circ\text{C}$  (green) and when temperature increment is consider (blue)  
13 for a  $\text{NaYbF}_4:\text{Er}^{3+},\text{Nd}^{3+}$  microparticle. (d) Change in the intensity ratio as a function of the  
14 trapping power,(e) rotation rate as a function of the laser power and (f) trap stiffness as a  
15 function of the laser power when temperature is set to  $22^\circ\text{C}$  (green) and when temperature  
16 increment is consider (blue) for a  $\text{NaYF}_4:\text{Er}^{3+},\text{Yb}^{3+}$  microparticle. Where not present, error  
17 bars are smaller than the symbols denoting the data points.  
18  
19  
20  
21  
22

23 Figure 3: Temperature as a function of power measured for a  $\text{NaYbF}_4:\text{Er}^{3+},\text{Nd}^{3+}$  micropar-  
24 ticle by using the three thermometric methods: luminescence (green triangles), rotation rate  
25 (cyan circles), trap stiffness (navy squares). A room temperature of  $22^\circ\text{C}$  is assumed.  
26  
27  
28  
29  
30  
31  
32  
33  
34  
35  
36  
37  
38  
39  
40  
41  
42  
43  
44  
45  
46  
47  
48  
49  
50  
51  
52  
53  
54  
55  
56  
57  
58  
59  
60

## Graphical TOC Entry

